



# Product desorption limitations in selective photocatalytic oxidation

T.J.A. Renckens<sup>a,\*</sup>, A.R. Almeida<sup>b</sup>, M.R. Damen<sup>a</sup>, M.T. Kreutzer<sup>a</sup>, G. Mul<sup>b,\*</sup>

<sup>a</sup> Product and Process Engineering, Department of Chemical Engineering, Delft University of Technology, Delft, The Netherlands

<sup>b</sup> Catalysis Engineering, Department of Chemical Engineering, Delft University of Technology, Delft, The Netherlands

## ARTICLE INFO

### Article history:

Available online 18 January 2010

### Keywords:

Operando spectroscopy  
Transient experiments  
Unsteady-state processes  
Photocatalysis  
Attenuated Total Reflection Fourier Transform Infrared Spectroscopy (ATR FT-IR)  
Surface characterization

## ABSTRACT

The rate of photocatalytic processes can be significantly improved if strongly bound products rapidly desorb to free up active sites. This paper deals with the rate of desorption of cyclohexanone, the product of the liquid-phase photo-oxidation of cyclohexane. Dynamic step-response and pulse-response experiments were performed, and the interaction with a TiO<sub>2</sub> surface was monitored using ATR FT-IR spectroscopy. A key result is that cyclohexanone desorbs readily from unexposed surfaces and desorbs an order of magnitude slower from UV-illuminated titania. The modification of the surface by UV is reversible: after 2 h without UV illumination the surface behaves as an unexposed one. The spectroscopic data support an explanation where without illumination, the cyclohexanone adsorbs on surface-bound water, from which it readily desorbs. Illumination, on the other hand, converts part of this water to accessible hydroxyl groups on titania. Cyclohexanone, forming during illumination, binds to these Ti–OH groups, and consequently desorbs much slower.

© 2009 Elsevier B.V. All rights reserved.

## 1. Introduction

The key advantage of photocatalysis is that photonic energy rather than thermal energy is used to induce a surface reaction, allowing the chemistry to generally run at ambient conditions [1,2]. An associated downside is that at lower temperatures all reactants and products are bound much more strongly to the surface. This may induce desorption limitations [3], so understanding surface coverage in photocatalysis is crucial to rationally optimize the process conditions for a specific photocatalytic reaction.

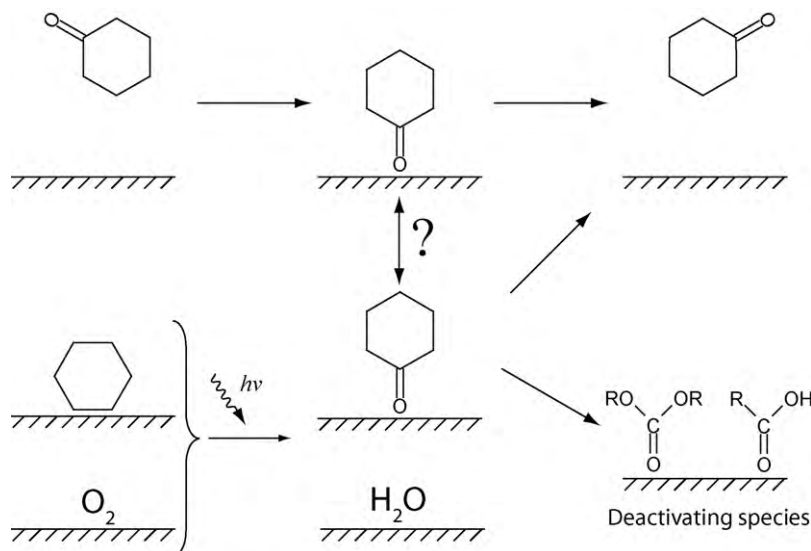
Temperature programmed desorption (TPD) [4,5] and surface plasmon resonance (SPR) [6] are widespread techniques to study the conversion and desorption behaviour of species present on catalyst surfaces. In TPD, a temperature gradient is used to sequentially desorb (or react) components, usually to an inert gas-atmosphere for analysis by GC or MS, and the rate of desorption at operating temperature is then estimated using a rate expression of the Arrhenius-type. In SPR, a change in refractive index is measured in time as material desorbs from the surface, usually in a flow that carries the desorbed material from the surface to prevent re-adsorption. SPR offers high flexibility in mimicking relevant operating conditions, including temperature and, importantly, solvents for liquid-phase processes.

Attenuated Total Reflection Fourier Transform Infrared (ATR FT-IR) spectroscopy resembles SPR, except that instead of a change in refractive index, a full infrared spectrum is recorded. In a dynamic experiment, the presence of species in a volume close to the surface (within a few  $\mu\text{m}$ ) can be recorded. This means that it is possible to obtain chemical information on catalyst coatings, species adsorbed on them and their surrounding media in a single experiment [7]. This technique has been applied to perform *operando* studies of heterogeneous catalysts in a variety of reactions and solvents [8–11]. By studying species in solution and species on the catalyst surface simultaneously in time, it is possible to determine desorption rates [12] in relevant solvents at the operating temperature without an extrapolation based on the Arrhenius equation.

In this work, we analyze the surface coverage of species involved in the selective photocatalytic oxidation of cyclohexane to cyclohexanone on a TiO<sub>2</sub> photocatalyst. The current process for cyclohexane oxidation is operated at elevated temperatures at low conversion (<0.15) to avoid over-oxidation and produces byproduct cyclohexanol. This process is very energy intensive due to temperature of operation and high separation duties [13]. Photocatalytic oxidation of cyclohexane runs at ambient conditions and is highly selective. It can thus offer an alternative that is less energy demanding. The biggest shortcoming of photocatalytic oxidations is that catalytic activity, though initially reasonably high, rapidly decreases [14], as product and deactivating species accumulate on the catalyst with time on stream [15] (see Scheme 1).

Several findings in the literature relate deactivation to the desorption behavior of cyclohexanone from titania. It has been

\* Corresponding authors at: Julianalaan 136, 2628 BL Delft, The Netherlands.  
Tel.: +31 15 289 43 81; fax: +31 15 278 50 06.  
E-mail address: [G.Mul@tudelft.nl](mailto:G.Mul@tudelft.nl) (G. Mul).



**Scheme 1.** The top row shows the adsorption/desorption process on the  $\text{TiO}_2$  surface. The bottom row shows the reactive process in which adsorbed cyclohexane reacts with adsorbed oxygen to photocatalytically form adsorbed cyclohexanone species and water or deactivating species. The main question that we address in this work is whether the two adsorbed cyclohexanone species are chemically identical and, if not, what the difference is.

found that improving product desorption by introducing a solvent, greatly improves catalyst activity and stability [16–18]. Water also plays an important role in the desorption characteristics of products formed on titania, as it forms a multilayer surface structure [19,20], and reacts under illumination to form additional surface hydroxyl groups, causing increased hydrophilicity [21,22]. Given the low operation temperature, product desorption in photocatalytic processes is probably limiting, as also observed for e.g. propylene oxide, the product in the thermally induced partial oxidation of propene over  $\text{Au/TiO}_2$  [23]. Understanding the desorption of cyclohexanone is key to improving titania stability and activity in photon induced selective oxidation of cyclohexane, and to optimize conditions for this promising photocatalytic process.

Our main contribution in this work is to compare desorption of cyclohexanone from illuminated titania in *operando* experiments with desorption from titania without any reaction (see Scheme 1). We find that the desorption rates are much slower for the case where there is photocatalytic activity. We show here experiments that unify these findings, and point in the direction of changes in the water environment of the catalyst surface upon illumination, to explain the observed phenomena.

The paper is organized as follows: we begin by explaining our spectroscopy flow cell and determine how fast we can switch conditions. This defines an experimental limit for the adsorption/desorption speeds that can be analyzed. We succinctly describe our main results, the time-evolution of adsorbed species for surfaces with different histories of exposure to UV light and external cyclohexanone in a flow of cyclohexane. We then characterize the peaks that we find in the experiments, and discuss the red shifts of the adsorbed species. Lastly, we interpret the results and offer a scheme that is in agreement with the combined spectroscopic evidence and dynamic behavior.

## 2. Experimental methods

### 2.1. Preparation and characteristics of the $\text{TiO}_2$ photocatalytic coating

The titania catalyst used in this work was present as a coating of agglomerated nanoparticles on top of the crystal used for ATR FT-IR spectroscopy. Hombikat UV100 (Sachtleben) was used as the titania photocatalyst and was heated to  $120^\circ\text{C}$  ( $5^\circ\text{C}/\text{min}$ ) in air before use. To prepare the coating, 1.4 g/L of calcined titania was

suspended in 30 mL of demineralized water and sonicated for 30 min. Subsequently, 2.5 mL of the suspension was pipetted onto the bottom plate of the flow cell (see Fig. 1), already containing the ATR crystal. The suspension was dried overnight at a pressure of 0.1–0.5 bar in a dessicator. This procedure yielded a coating of approximately  $8\text{--}10\ \mu\text{m}$  thick that adhered to the ATR crystal. Afterwards, the coating was dried further at  $120^\circ\text{C}$  for 1 h before use to remove part of the surface water. Even though we expected some water to be present on the catalyst surface, we chose not to dry at higher temperature because higher temperature treatment would permanently alter the catalyst [14].

### 2.2. Experimental ATR FT-IR setup

The ATR FT-IR setup consisted of a Harrick Horizon multiple internal reflections accessory coupled to a 4 mL flow cell containing a ZnSe ATR crystal (see Fig. 1), as described elsewhere [15]. The Fourier transform infrared measurements were performed on a

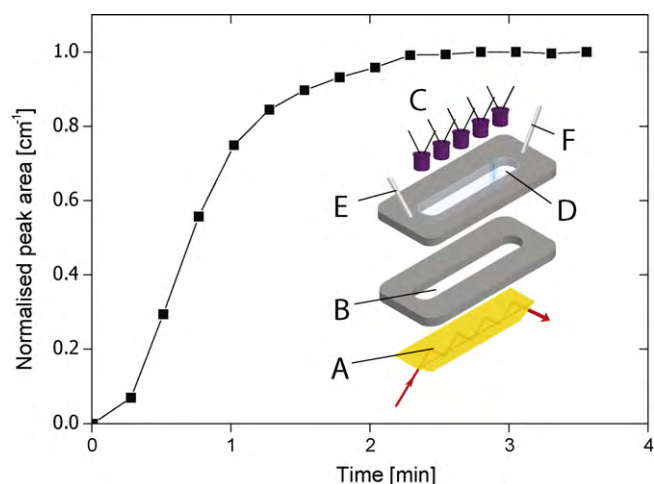


**Fig. 1.** Experimental setup, showing the ATR crystal (A), the chamber of the ATR flow cell (B), the array of UV LED's (C) used to illuminate the catalyst through a Quartz window (D), and the fluid inlet (E) and outlet (F). The graph shows the response of the ATR signal to a step change in concentration of cyclohexanone from 0 to 0.05 M at the inlet.

Nicolet 8700 FT-IR equipped with a TRS detector cooled with a liquid  $N_2$ . A mirror velocity of 1.8988 cm/s and a resolution of  $4\text{ cm}^{-1}$  were used for all measurements. The background and the sample spectra were averaged from 64 to 32 spectra, respectively. In some cases, measurements were averaged further to improve signal to noise ratio.

### 2.3. Conditions of flow-through experiments

Reagent grade cyclohexanone (99%, Aldrich) and reagent grade cyclohexanone (99.5%, Aldrich) were dried using molecular sieves to reduce the water content unless stated otherwise. Cyclohexanone saturated with water was prepared by vigorously shaking a two phase water and cyclohexanone system, sonicating it for 15 min, allowing the obtained emulsion to separate over 2 days and withdrawing the cyclohexanone phase. In all cases, cyclohexanone was flowed over the catalyst coating for at least 2 h prior to experimentation to reach a stable level of adsorbed water and cyclohexanone. A new catalyst coating was prepared for each experiment, unless explicitly mentioned, to rule out the effect of possible changes in catalyst surface (e.g. deactivating species or residual cyclohexanone).

Because our key experiments determined the time response to a step change, we first evaluated the time response to a step change for a flow cell without any catalyst coating. This response captured all the phenomena that we were not explicitly interested in, such as mass transfer to the crystal, hydrodynamic dispersion inside the cell and hydrodynamic dispersion in the feed lines. A step change in the feed from 0 to 0.05 M cyclohexanone in cyclohexanone was imposed. The experiment was carried out in flow-through mode and solutions were dispensed using a Harvard PhD2000 syringe pump at 4 mL/min.

For desorption of externally fed cyclohexanone, both on fresh catalyst and catalysts exposed to UV illumination, a 0.05 M solution of cyclohexanone in cyclohexanone, or alternatively in water saturated cyclohexanone, was flowed for 15 min to adsorb cyclohexanone. Afterwards, the desorption was performed by switching to pure cyclohexanone, or water saturated cyclohexanone, respectively. The background used for recording spectra was recorded prior to the adsorption of cyclohexanone on the  $TiO_2$  coating. In all cases, solutions were dispensed using a Harvard PhD2000 syringe pump at 4 mL/min.

The desorption of *in situ* formed cyclohexanone was carried out in approximately 100 mL of recirculating cyclohexanone—for our experiments this was equivalent to a flow-through system. Cyclohexanone was saturated with oxygen by bubbling dry air at 7.7 mL/min flow for 1 h. The oxygen-saturated cyclohexanone was circulated at 4 mL/min through the ATR cell by means of a series-II high performance liquid chromatography pump. The photocatalytic reaction was initiated for 2 min by a bank of 7 UV LEDs (Roithner Lasertechnik), producing 375 nm light at  $9 \times 10^{-9}\text{ Einstein cm}^{-2}\text{ s}^{-1}$ . A 0.4 mL sample loop was placed between the aeration vessel and the flow cell, allowing the introduction of 0.03 M cyclohexanone solved in cyclohexanone during the experiment. The background spectrum was recorded before initiation of the photocatalytic reaction.

### 2.4. Processing and interpretation of obtained IR spectra

To enable quantitative analysis of the individual absorption peaks making up the infrared spectra measured, the spectra were deconvoluted using a custom MATLAB routine. This routine performed a horizontal baseline correction of the spectrum and subsequently individual peaks of the Voigt profile were combined into a composite calculated spectrum. This calculated spectrum was fitted to the measured spectrum using a routine

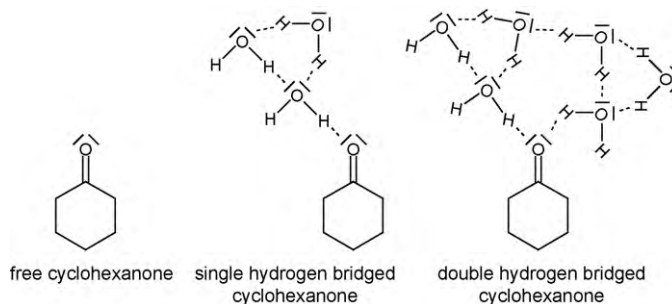
that performed a nonlinear least squares curve fit, using peak position, height and width of the individual peaks as fit parameters.

Spectra obtained were deconvoluted into the following individual contributions as described below. In the experiment to determine mass transfer in the flow cell, cyclohexanone in solution was deconvoluted into two contributions at 1720 and  $1711\text{ cm}^{-1}$ . For cyclohexanone desorption experiments, spectra obtained between 1800 and  $1500\text{ cm}^{-1}$  were deconvoluted as seven contributions at  $\sim 1720$ ,  $\sim 1700$ ,  $\sim 1680$ ,  $\sim 1650$ ,  $\sim 1625$ ,  $\sim 1580$  and  $\sim 1525\text{ cm}^{-1}$ . The peak at  $1720\text{ cm}^{-1}$  was assigned to cyclohexanone in solution and the peak at  $1680\text{ cm}^{-1}$  was assigned to adsorbed cyclohexanone [15]. The peak at  $1700\text{ cm}^{-1}$  was assigned to a second specie of adsorbed cyclohexanone—this assignment will be discussed further in this work. The peaks at 1650 and  $1625\text{ cm}^{-1}$  were assigned to water bending modes, both as a negative peak in the case that the water presence diminishes, and as an isosbestic point. The isosbestic point represents a positive and a negative contribution of approximately the same intensity at wavenumbers that lie close together, in this case caused by a change in water O–H bending vibration due to a change in the water molecule surroundings. Because this contribution would change from an isosbestic to a negative peak, deconvolution of these peaks was sometimes unstable. In practice, this meant that the deconvolutions would jump between two competing solutions of the least squares optimization, showing up as increased noise in the deconvoluted peak areas. These peaks were therefore only used to improve the deconvolution of other peaks and not to draw conclusions. The peaks at 1580 and  $1525\text{ cm}^{-1}$  were assigned to carboxylate surface species [15].

To deconvolute the spectra between 4000 and  $3050\text{ cm}^{-1}$  obtained during cyclohexanone desorption experiments, peaks at  $\sim 3640$ ,  $\sim 3400$ , and  $\sim 3200\text{ cm}^{-1}$  were used. The broad feature was deconvoluted with only two peaks, as more peaks would destabilize the deconvolution. The vibration at  $\sim 3640\text{ cm}^{-1}$  was attributed to titania surface hydroxyl groups. The broad feature between 3700 and  $3050\text{ cm}^{-1}$  was attributed to absorption by a combination of water and surface hydroxyl groups hydrogen bonded to another molecule [24].

### 2.5. Molecular modeling of hydrogen bridged cyclohexanone

The position of the C=O stretch vibration of cyclohexanone was interpreted using molecular modeling for three different cases. All molecular modeling was carried out using the Spartan'06 molecular modeling suite of programs. First, cyclohexanone and water molecules were geometrically optimized using a semi-empirical PM3 approach. Finally, the IR spectra were obtained from



**Scheme 2.** This scheme shows a 2D representation of the situations modeled using molecular modeling. Case one is free cyclohexanone in vacuum. Case two is cyclohexanone hydrogen bound to one water molecule, which in turn is hydrogen bound with two other water molecules. Case three is a cyclohexanone with two hydrogen bonds to two different water molecules, both of which have hydrogen bridges to two other water molecules.

energy optimizations performed at the EDF1/6-31G\* level. In a first simulation, cyclohexanone was isolated. In the second case, the ketone group of cyclohexanone was hydrogen bonded to a water molecule, which in turn was hydrogen bonded to two other water molecules. In a third case, the ketone group of cyclohexanone was hydrogen bonded to two water molecules, both of which were hydrogen bonded to two other water molecules. These three situations are shown in Scheme 2 as a two dimensional representation.

### 3. Results

#### 3.1. Step change experiment in flowcell without catalyst coating

The response to a step change in the feed from 0 to 0.05 M cyclohexanone in cyclohexane is shown in Fig. 1. The cyclohexanone peak (see below) gradually increases until it reaches the final concentration after approximately 2.5 min.

#### 3.2. Desorption of cyclohexanone from titania not exposed to UV light

To determine the desorption rate of cyclohexanone not exposed to UV light from a fresh catalyst, the flow was changed from a

cyclohexanone solution to pure cyclohexane. During the desorption of cyclohexanone, one peak associated with cyclohexanone in solution ( $1722\text{ cm}^{-1}$ ) and two species of adsorbed cyclohexanone ( $1697$  and  $1679\text{ cm}^{-1}$ ) are observed (see Fig. 2a). All three peaks decrease during the experiment, because the adsorbed cyclohexanone desorbs and because the desorbed cyclohexanone in solution is flushed out of the flow cell. Fig. 2b shows that the time it takes for 90% of the adsorbed cyclohexanone to desorb is 5.5 min for adsorbed cyclohexanone species I and 6.1 min for adsorbed cyclohexanone species II. In comparison to a switch in an empty channel, the process takes twice as long. After desorption, a residual of strongly bound cyclohexanone species II is present (Fig. 2b).

During cyclohexanone desorption, spectra were also collected in the  $4000\text{--}3050\text{ cm}^{-1}$  region, where information about OH stretch vibrations is found (see Fig. 3a). Surface hydroxyl groups ( $3633\text{ cm}^{-1}$ ) are shown to return to the level prior to cyclohexanone adsorption. The broad feature between  $3600$  and  $3050\text{ cm}^{-1}$ , attributed to water and surface hydroxyl groups hydrogen bonded to another molecule, first decreases and afterwards stabilizes. By comparing Figs. 2b and 3b, the combined adsorption of hydrogen bonded surface hydroxyls and water is seen to decrease with the desorption of cyclohexanone. Conversely, the surface hydroxyl groups restore upon the desorption of cyclohexanone.

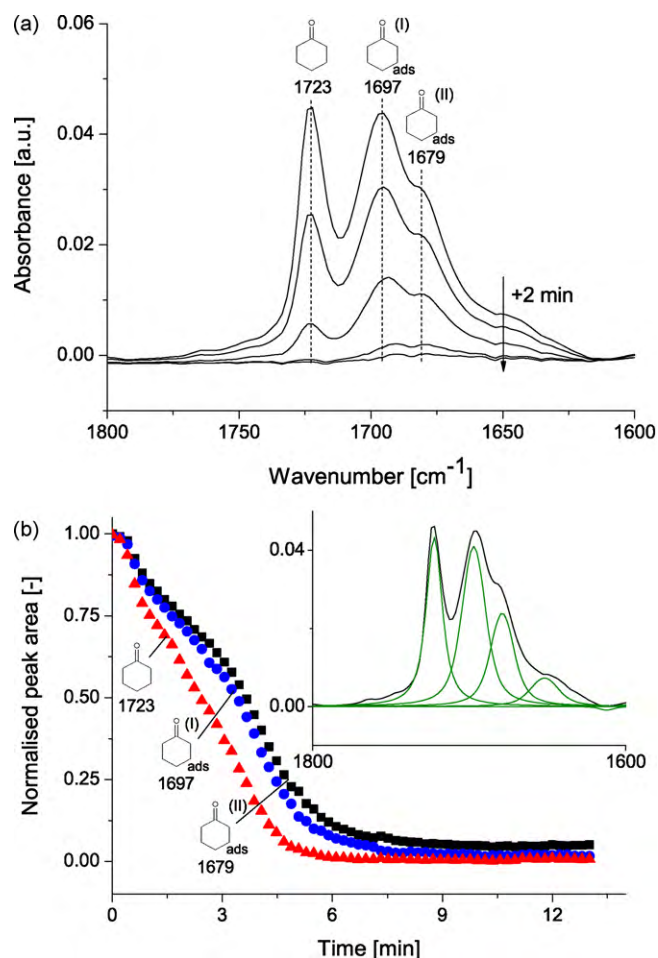


**Fig. 2.** (a) Full spectra and (b) evolution of deconvoluted peak areas after a step change at  $t = 0$  at the inlet of the flow cell from 0.05 M to 0 M cyclohexanone in cyclohexane. The inset in (b) shows the deconvoluted peaks and a raw spectrum. In the spectra, one peak for cyclohexanone is in solution and two peaks are assigned to adsorbed cyclohexanone adsorbed on two different sites. Note that both these peaks decrease in time almost as fast as the peak of cyclohexanone present in the bulk.

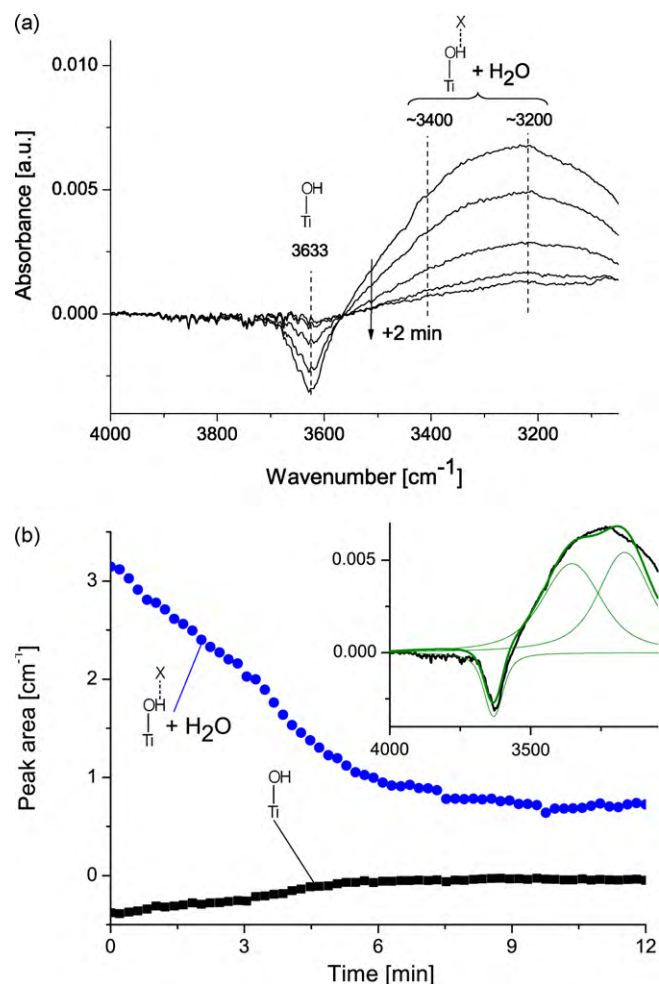


**Fig. 3.** (a) Full spectra and (b) evolution of deconvoluted peak areas after a step change at  $t = 0$  at the inlet of the flow cell from 0.05 M to 0 M cyclohexanone in cyclohexane. The inset in (b) shows the deconvoluted peaks and a raw spectrum. In the spectra, one peak is assigned to free surface hydroxyl groups and the broad feature is assigned to a combination of hydrogen bonded hydroxyls and water. Note that both these peaks have similar, if opposite, trends.



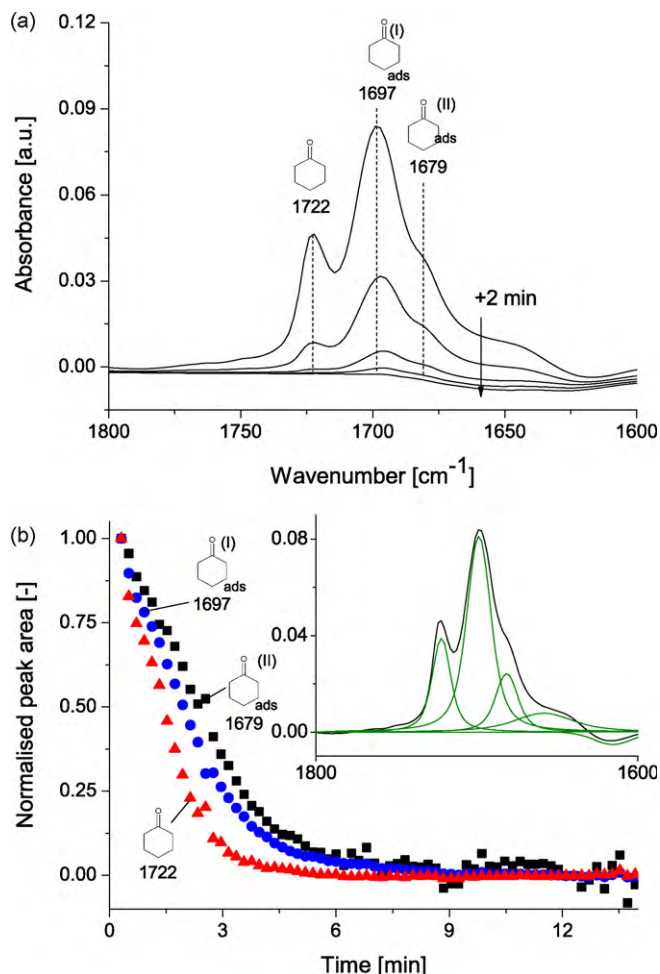


**Fig. 4.** (a) Full spectra and (b) evolution of deconvoluted peak areas after a step change at  $t = 0$  at the inlet of the flow cell from 0.05 M to 0 M cyclohexanone in water saturated cyclohexane. The inset in (b) shows the deconvoluted peaks and a raw spectrum. In the spectra, one peak for cyclohexanone is in solution and two peaks are assigned to adsorbed cyclohexanone adsorbed on two different sites. Note that the amount of adsorbed cyclohexanone is higher compared to the case where the solvent is dried with molsieves.

### 3.3. Desorption of cyclohexanone from titania not exposed to UV light in water saturated cyclohexane

This experiment was similar to the one described above, but instead of molsieve dried cyclohexane, cyclohexane saturated with water was used as a solvent. The flow was changed from an 0.05 M solution of cyclohexanone in this solvent to a 0 M solution. Peaks for cyclohexanone in solution and for the two species of adsorbed cyclohexanone were observed and, as seen in Fig. 4a, decrease in time. Fig. 4b shows the peak areas obtained by deconvolution. 90% of the adsorbed cyclohexanone species I desorbs in 4.0 min, and 90% of the adsorbed cyclohexanone species II desorbs in 4.5 min. This is faster than compared to the situation where molsieve dried cyclohexane was used as solvent.

### 3.4. Desorption of cyclohexanone from titania formed by photocatalytic oxidation

Now we consider an experiment in which cyclohexanone is not adsorbed on the surface, but formed in a photocatalytic reaction. After illuminating the catalyst for 2 min under cyclohexane flow, two peaks associated with species of *in situ* formed adsorbed cyclohexanone appear (see Fig. 5a). In contrast to the experiments

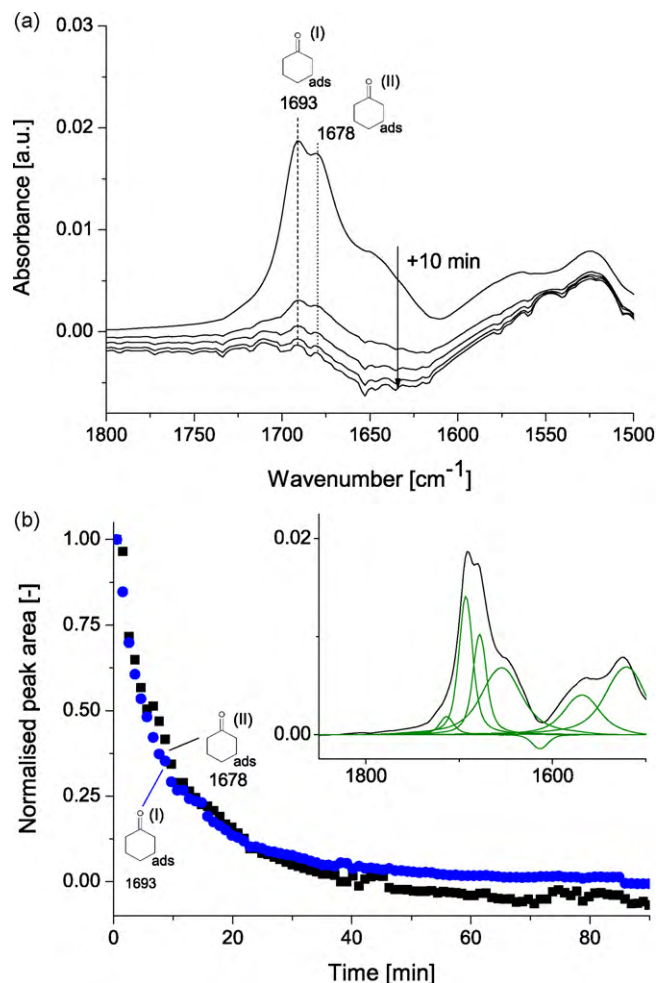


**Fig. 5.** (a) Full spectra and (b) evolution of deconvoluted peak areas after a 2 min period of illumination in a flow cell that was continuously fed with cyclohexane. The spectra were recorded in the dark. The inset in (b) shows the deconvoluted peaks and a raw spectrum. During the 2 min of illumination, cyclohexanone is formed on the surface. The spectra show the formation of two species of adsorbed cyclohexanone. The time at which 90% of the desorption was complete was 22.8 min and 29.5 min for species I and species II, respectively.

above, broad features below 1600 cm<sup>-1</sup> indicating deactivating species [15] are visible and the range of wavenumbers has been increased to show these features. We did not observe a significant peak for free cyclohexanone. The peak positions of the adsorbed cyclohexanone are more shifted towards the red (5 cm<sup>-1</sup> for species I and 2 cm<sup>-1</sup> for species II) than the previously described externally fed cyclohexanone. The most dramatic difference is not the red shift, however. The desorption times in this experiment, where cyclohexanone is formed photocatalytically, are significantly longer (see Fig. 5b). The times for 90% cyclohexanone desorption are 22.8 ± 1 min (species I) and 29.5 ± 1 min (species II).

### 3.5. Desorption of cyclohexanone from titania that was exposed to UV light 5 min before adsorption

The previous two experiments clearly showed that cyclohexanone desorbs much more slowly in a photocatalytic process than from titania not exposed to UV light. To further understand the nature of this difference, we executed a third experiment in which some cyclohexanone is formed under illumination of the surface for 2 min, followed by switching off the light and, 5 min later, introduction of a pulse of 0.03 M cyclohexanone solution into the flow cell. The IR spectra recorded are shown in Fig. 6a.

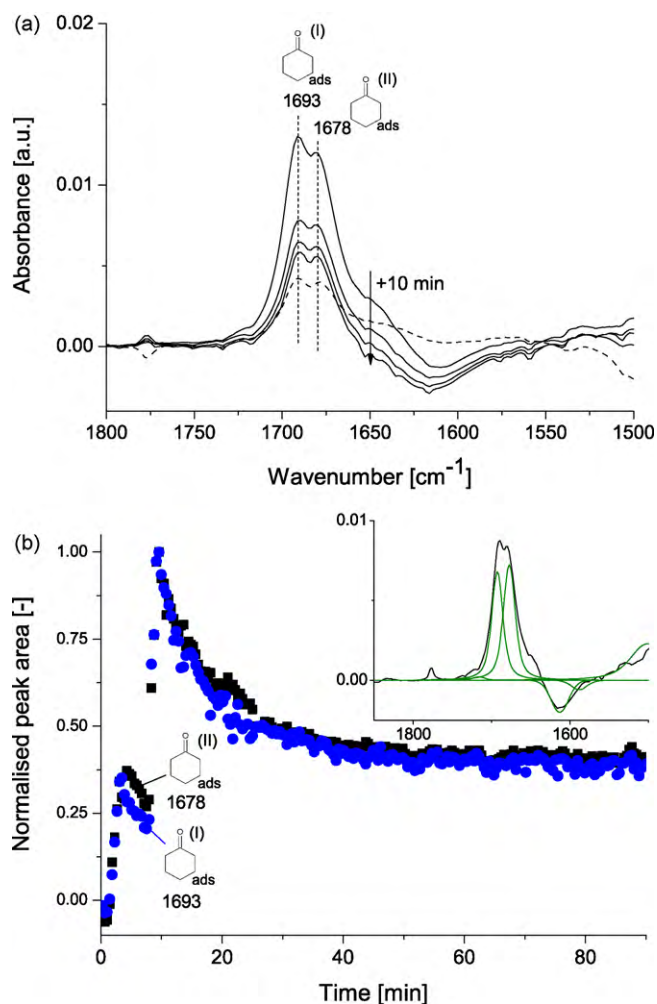


**Fig. 6.** (a) Full spectra and (b) evolution of deconvoluted peak areas of a 2 min period of illumination at  $t = 1$  min in a flow cell that was continuously fed with cyclohexanone. Five minutes after illumination at  $t = 8$  min, 0.4 mL of 0.03 M cyclohexanone solution was fed. (a) The spectrum after 2 min of illumination (dotted line) and the spectrum after adsorption of externally fed cyclohexanone (bold line). The inset in (b) shows the deconvoluted peaks and a raw spectrum. During the 2 min of illumination, cyclohexanone is formed on the surface. The spectra show the formation of two species of adsorbed cyclohexanone. The time at which 90% of the desorption was complete was 22.1 min and 22.6 min for species I and species II, respectively. Note that 40% of the adsorbed cyclohexanone species do not desorb.

The cyclohexanone introduced in this pulse significantly adsorbs on the surface, as shown in Fig. 6b. The rate of desorption of externally fed cyclohexanone on a preilluminated surface is very similar to that of *in situ* formed by conversion of cyclohexane. The times for 90% cyclohexanone desorption were  $21.1 \pm 0.4$  min (species I) and  $21.6 \pm 0.4$  min (species II). Another remarkable feature is that  $\sim 40\%$  of the adsorbed cyclohexanone did not leave the surface after adsorption. It should be noted that an exception is made in this experiment in the number of contributions used to deconvolute the spectra. The  $1650\text{ cm}^{-1}$  peak was causing instability in the deconvolution and was therefore left out. This has no effect on the observed phenomena indicated above.

Fig. 7a shows the band dynamics in the spectral region of the OH stretch vibrations for the above experiment. A negative OH stretch vibration at around  $3640\text{ cm}^{-1}$ , attributed to surface hydroxyl groups, is seen to partially recover from an initial decrease. The broad feature between  $3700$  and  $3050\text{ cm}^{-1}$ , attributed to water and surface hydroxyl groups hydrogen bonded to another molecule, initially increases and afterwards decreases and stabilizes at an absorption value lower than recorded in the

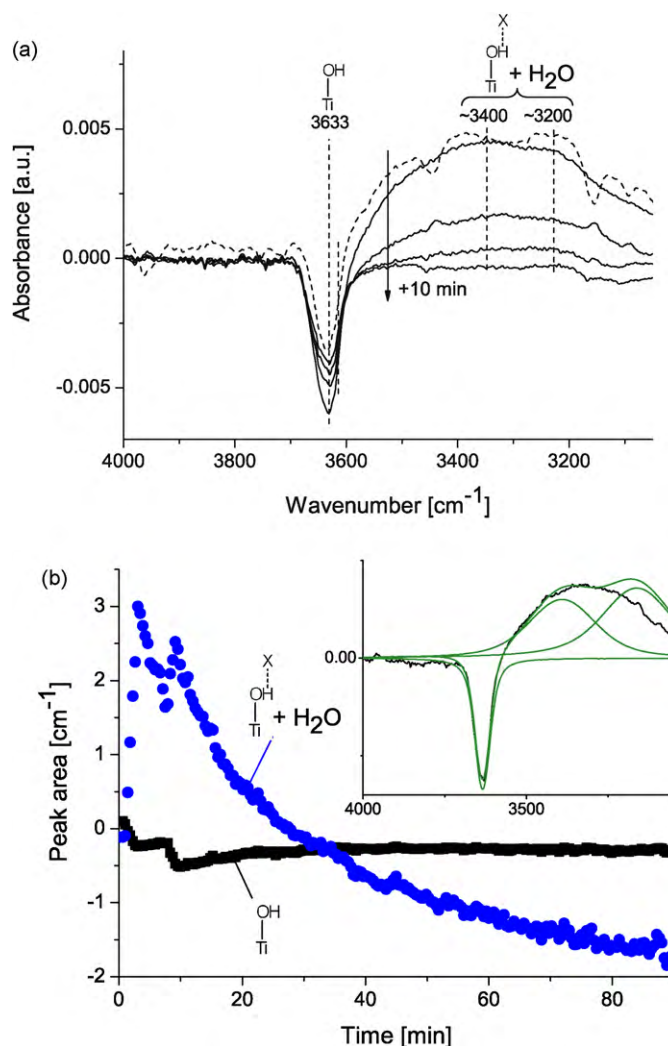


**Fig. 7.** (a) Full spectra and (b) evolution of deconvoluted peak areas of a 2 min period of illumination at  $t = 1$  min in a flow cell that was continuously fed with cyclohexanone. Five minutes after illumination at  $t = 8$  min, 0.4 mL of 0.03 M cyclohexanone solution was fed. (a) The spectrum after 2 min of illumination (dotted line) and the spectrum after adsorption of externally fed cyclohexanone (bold line). The inset in (b) shows the deconvoluted peaks and a raw spectrum. Note that 40% of the consumed titania hydroxyls is not restored.

background. Comparison of Figs. 6b and 7b shows that the surface hydroxyl group intensity increases upon desorption of cyclohexanone; both stabilize at levels of  $\sim 40\%$  of their minimum and maximum signal, respectively.

### 3.6. Desorption of cyclohexanone from titania that was exposed to UV light 2 h before adsorption

Desorption of cyclohexanone from a  $\text{TiO}_2$  coating 2 h after that coating was used for photocatalysis, is shown in Fig. 8a. The result is very similar to the result obtained for a surface that was never illuminated (Fig. 2a). From Fig. 8b, the time for 90% desorption can be determined as  $8.8 \pm 0.2$  min and  $9.3 \pm 0.2$  min, compared with  $\sim 6$  min for the unilluminated surface.

### 3.7. Molecular modeling of hydrogen bridged cyclohexanone

The results of our modeling effort are shown in Table 1. Because the absolute value of calculated spectra is not accurate, only the shifts relative to the base case of free cyclohexanone are reported.

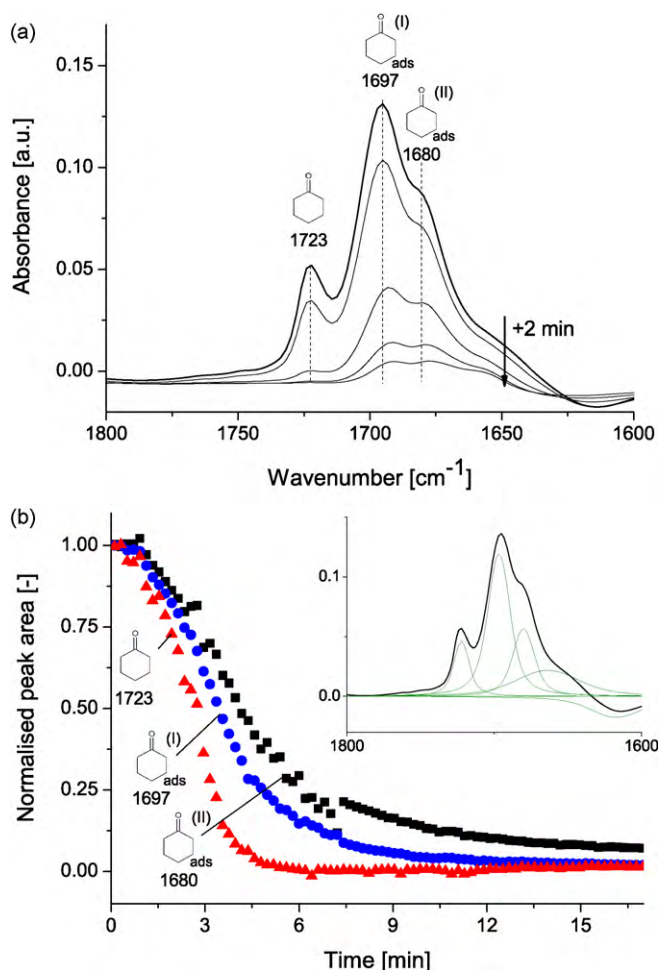


**Fig. 8.** (a) Full spectra and (b) evolution of deconvoluted peak areas executed after the experiment shown in Fig. 5. As in Fig. 4, this figure shows the response to a step change at  $t = 0$  at the inlet of the flow cell from 0.05 M to 0 M cyclohexanone in cyclohexane. The inset in (b) shows the deconvoluted peaks and a raw spectrum. The behavior is very similar to that shown in Fig. 3, except that cyclohexanone desorption is somewhat slower, but still much faster than of species desorbing from an illuminated catalyst shown in Figs. 5 and 6.

The formation of one and two hydrogen bonds leads to a red shift of  $\sim 22$  and  $\sim 36$   $\text{cm}^{-1}$ , respectively. This corresponds with the red shifts that we observe for the two peaks associated with adsorbed species.

#### 4. Discussion

Before we discuss the results in depth, we remark here that the experimental method is highly useful to study desorption limitations in heterogeneous (photo-)catalysis. It is crucial to perform the experiments *operando*, with the ability to rapidly introduce reactants and products while the surface is catalytically active. Post-mortem experiments on photocatalysts outside a reactor, for instance TPD, would have to be performed rapidly after

illumination not to allow the surface to revert back to its unilluminated state. The fact that we obtain full spectra, instead of only a broad measure of surface coverage as would be obtained from surface plasmon resonance, is essential in allowing the discussion that follows below.

The step change experiment in the empty flowcell is completed in 2.5 min. We can therefore only measure true desorption characteristics if they are slower than the response time of the cell. If faster, all we will be able to say is that desorption processes are fast with respect to the 2 min response time of the cell.

Table 2 summarizes the desorption times of cyclohexanone for different cases. The two different species of adsorbed cyclohexanone have very similar desorption times. This means that these two species adsorb with very similar adsorption strengths or exchange rapidly. Our molecular modeling results (Table 1) indicate that we can explain the presence of two bands for adsorbed cyclohexanone as single and double hydrogen bridged cyclohexanone. Because hydrogen bridges are generally low energy bonds, rapid exchange is possible. In summary, we propose that adsorbed cyclohexanone exchanges rapidly between a single and double hydrogen bonded state. This also explains why both species show similar desorption rates.

We also examined our cyclohexanone desorption data to see if any coverage effects, i.e. deviation from the Langmuir assumption that all sites are equal [25], were present. If no coverage effect is present, desorption is a first-order phenomenon and it will follow an exponential decay. In the case where concentration in solution is low and no adsorption takes place in addition to desorption, this is easily verified by plotting the data on a semi-log scale (not shown). For our experiments where we could perform this analysis, no coverage effects were found.

The experiments show directly that slow product desorption occurs due to changes in the catalyst surface upon illumination. It does not matter whether cyclohexanone is fed right after illumination externally, or is formed on the surface. Additionally, from our desorption experiments from titania that was exposed to UV light 2 h before adsorption, we can conclude that the change in cyclohexanone desorption rate caused by illumination, is reversible. Slower desorption should therefore not be attributed to permanent changes of the catalyst, such as the formation of deactivating species. The desorption experiment using water saturated cyclohexane as a solvent suggests water plays an important role in determining desorption rate. We are not aware of any other work that clearly shows and discusses this difference in desorption rates due to illumination of a photocatalyst.

We now discuss the spectral information in detail. It can be expected that the stronger the binding of the molecule to the catalyst surface, the more the molecular vibration will change. The 1800–1500  $\text{cm}^{-1}$  region of the IR spectra (Figs. 2a, 4a, 5a, 6a and 8a) shows that the peak position for cyclohexanone bound with a single hydrogen bond ( $1697$   $\text{cm}^{-1}$ ) is different from photocatalytically formed cyclohexanone ( $1693$   $\text{cm}^{-1}$ ). In view of the small extent of this peak shift, the order of magnitude change in desorption rate is remarkable. The peak shift, if any, is even smaller for the molecules with two hydrogen bonds to the surface ( $1680$   $\text{cm}^{-1}$  versus  $1679$   $\text{cm}^{-1}$ ). Likewise, the infrared spectrum

**Table 1**

Red shifts of the cyclohexanone C=O stretch vibration; comparison of experimental observations with molecular modeling predictions. The experimentally observed shifts for the two species of adsorbed cyclohexanone (from cyclohexanone in solution onto an unilluminated surface, as in Fig. 3a) are compared with computational predictions for the shift in the case that cyclohexanone is hydrogen bonded to one or two water molecules from to the case of isolated cyclohexanone.

	Peak shifts		
	Experimental	Modeling	
Adsorbed species I	−26 cm <sup>−1</sup>	−22.0 cm <sup>−1</sup>	Single hydrogen bonded cyclohexanone
Adsorbed species II	−44 cm <sup>−1</sup>	−36.4 cm <sup>−1</sup>	Double hydrogen bonded cyclohexanone



**Table 2**

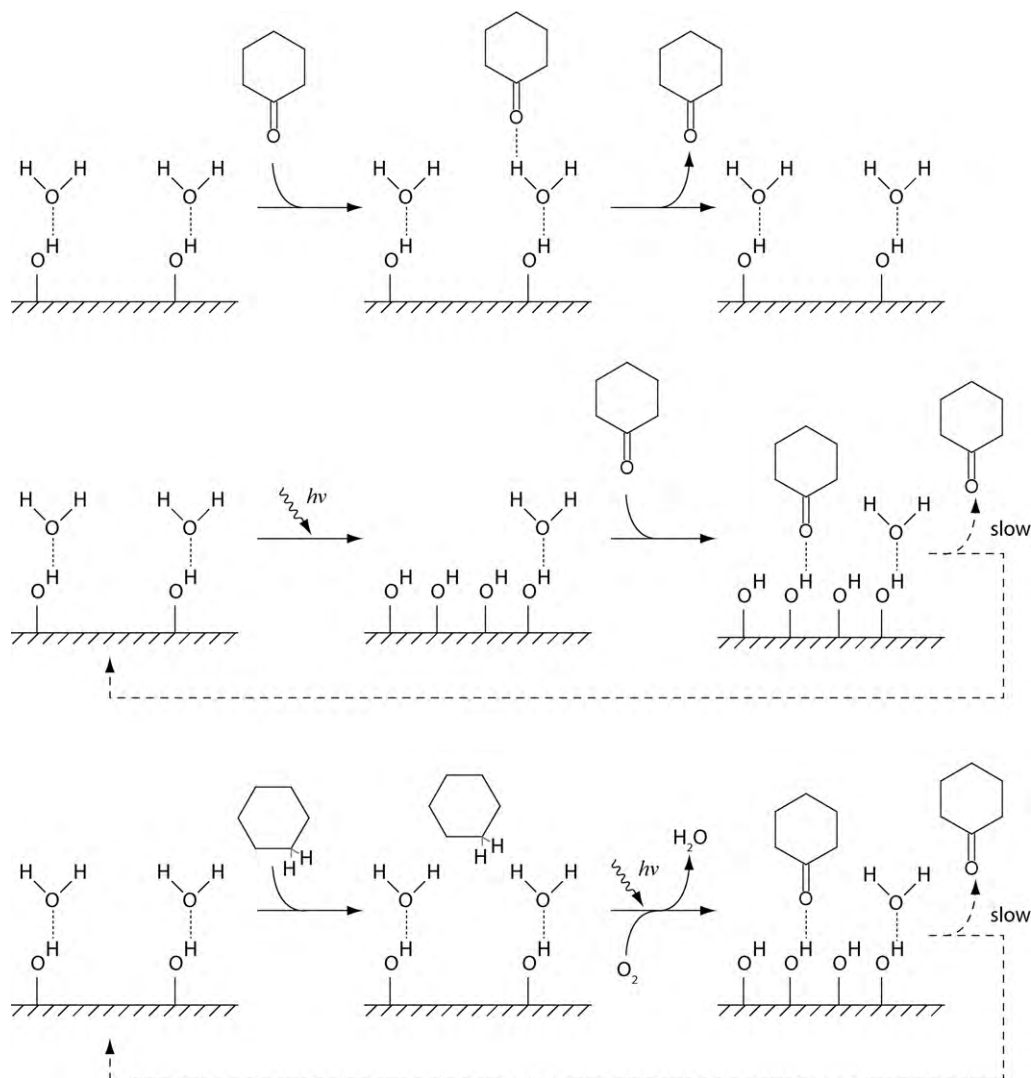
Time at which 90% of the transient is completed estimated from adsorption and desorption experiments. The level was determined from raw data and the measurement time interval is used as error estimation.

	Cyclohexanone (species I)	Cyclohexanone (species II)
Desorption of cyclohexanone from titania not exposed to UV light in a water saturated solvent	$4.0 \pm 0.2$ min	$4.9 \pm 0.2$ min
Desorption of cyclohexanone from titania not exposed to UV light	$5.5 \pm 0.2$ min	$6.1 \pm 0.2$ min
Desorption of cyclohexanone from titania that was exposed to UV light 2 h before adsorption	$8.8 \pm 0.2$ min	$9.3 \pm 0.2$ min
Desorption of cyclohexanone from titania that was exposed to UV light 5 min before adsorption	$21.1 \pm 0.4$ min	$21.6 \pm 0.4$ min
Desorption of cyclohexanone from titania formed by photocatalytic oxidation	$22.8 \pm 1$ min	$29.5 \pm 1$ min

of residual cyclohexanone (Fig. 6a) does not provide information on why this species is so strongly bound. As we have no further information on residual cyclohexanone, we will not speculate about its nature. In summary, the binding strength of the adsorbed species does not correlate very strongly with peak position.

When comparing adsorption of cyclohexanone in a dried solvent and in a water saturated solvent (Figs. 2a and 4a), a doubling of the peak height for adsorbed cyclohexanone species I is observed. This implies that an increase in water content allows for increased cyclohexanone adsorption and that cyclohexanone can interact with the water layer associated with the titania surface.

From the 4000 to 3050  $\text{cm}^{-1}$  region of the IR spectra (Figs. 4a and 7a), it can be seen that cyclohexanone adsorption affects the titania surface hydroxyl groups. Also in other work [24] it could be seen that a reduction of absorption at 3640  $\text{cm}^{-1}$  is compensated by the appearance of broader features at lower wavenumbers if a species is adsorbed on the  $\text{TiO}_2$  surface. The appearance of broader features does not match the behavior of the 3640  $\text{cm}^{-1}$  peak exactly, but this is due to changing concentrations of water. Remarkably, if water molecules are interposed between the cyclohexanone and the titania surface hydroxyl, the titania surface hydroxyl is still affected by the distant cyclohexanone, as we



**Scheme 3.** This scheme shows three different ways to create adsorbed cyclohexanone species. For clarity, the water layer, which may consist of several layers, is shown as a monolayer. The top row shows cyclohexanone adsorption in the dark, with water covering all surface hydroxyls and cyclohexanone adsorbs on the water layer. Cyclohexanone adsorbed on the water layer can readily desorb. The second row shows cyclohexanone adsorption after illumination. In this situation additional surface hydroxyl groups have been formed and cyclohexanone can adsorb on a titania surface hydroxyl directly. The same type of adsorbed cyclohexanone is formed in photocatalytic oxidation of cyclohexanone. Cyclohexanone adsorbed directly on the titania is more tightly bound than cyclohexanone adsorbed on the water layer and therefore desorbs more slowly.



observe in our spectra. This is in agreement with various studies reporting on the adsorption of organics on TiO<sub>2</sub> (e.g. [12,26]). The results suggest that, if water is present, organics may adsorb on the water layer instead of directly on the titania surface, but that this difference in adsorption mode will not have significant impact on changes in the OH-region of the infrared spectrum.

Based on the discussion above, we arrive at a possible explanation for the relatively large difference in desorption rate shown in Scheme 3. Titania is surrounded by layers of both weakly and strongly bound water, when cyclohexanone adsorbs onto titania not exposed to UV light, the amount of water is high enough to cover the surface hydroxyls, preventing cyclohexanone from adsorbing directly on the catalyst surface. In this case, cyclohexanone adsorbs by interaction with the water layer surrounding the catalyst. However, when the catalyst is illuminated, exposed surface hydroxyls become available and cyclohexanone can bind more strongly to the catalyst surface, resulting in slow desorption. For photocatalytic oxidation, the adsorbed cyclohexanone formed is also adsorbed directly on the OH-groups of the titania surface. Photocatalytically formed cyclohexanone therefore also shows lower desorption rates compared to cyclohexanone adsorbed onto titania not exposed to UV light.

## 5. Conclusion

We have determined the rate of desorption for cyclohexanone in cyclohexane from TiO<sub>2</sub> surfaces. We exposed the TiO<sub>2</sub> surface to externally fed cyclohexanone and cyclohexanone produced under UV illumination and studied the surface using a combination of transient reactor operation and operando spectroscopy. This study is the first to report that cyclohexanone desorbs significantly slower from an illuminated catalyst compared to cyclohexanone desorbing from a surface that has not been exposed to UV illumination.

The two adsorbed species of cyclohexanone observed in the infrared spectra were attributed to single and double hydrogen bonded cyclohexanone, but adsorption on different types of hydroxyl groups causes little difference in the infrared peak position. The presence of surface water increases the desorption rate.

Neither the origin of the cyclohexanone nor the presence of deactivating species causes the different desorption behavior. Rather, it is the amount of surface water relative to the titania surface hydroxyls. The illumination history of the surface is the dominating factor influencing this ratio.

UV illumination (partially) converts the adsorbed water layer into titania surface hydroxyls, allowing for stronger adsorption of cyclohexanone. All our experimental results agree with a hypothesis that the stronger adsorption of cyclohexanone occurs on these titania surface hydroxyls.

This study could only be possible using a combined transient operando spectroscopic approach.

## Acknowledgements

The authors would like to gratefully acknowledge Joana Carneiro, Roel van de Krol (both TU Delft) and Heinz Frei (Lawrence Berkeley National Laboratory) for insightful discussions on the cyclohexanone desorption behavior. This work was supported by ACTS (PoaC project 053.65.006) and STW (VIDI project DPC.7065).

## References

- [1] J.M. Herrmann, Topics in Catalysis 34 (2005) 49.
- [2] A.L. Linsebigler, G.Q. Lu, J.T. Yates, Chemical Reviews 95 (1995) 735.
- [3] W. Mu, J.M. Herrmann, P. Pichat, Catalysis Letters 3 (1989) 73.
- [4] S.A. Larson, J.A. Widegren, J.L. Falconer, Journal of Catalysis 157 (1995) 611.
- [5] D.S. Muggli, J.T. Mccue, J.L. Falconer, Journal of Catalysis 173 (1998) 470.
- [6] H.J. Lee, et al. Langmuir 21 (2005) 4050.
- [7] T. Burgi, A. Baiker, Advances in Catalysis 50 (50) (2006) 227.
- [8] I. Dolamic, T. Burgi, Journal of Catalysis 248 (2007) 268.
- [9] S.D. Ebbesen, B.L. Mojet, L. Lefferts, Journal of Physical Chemistry C 113 (2009) 2503.
- [10] C. Mondelli, et al. Journal of Catalysis 252 (2007) 77.
- [11] A. Urakawa, R. Wirz, T. Burgi, A. Baiker, Journal of Physical Chemistry B 107 (2003) 13061.
- [12] A.G. Young, A.J. McQuillan, Langmuir 25 (2009) 3538.
- [13] G. Franz, R.A. Sheldon, Ullmann's Encyclopedia of Industrial Chemistry, Wiley Interscience, New York, 2005.
- [14] P. Du, J.A. Moulijn, G. Mul, Journal of Catalysis 238 (2006) 342.
- [15] A.R. Almeida, J.A. Moulijn, G. Mul, Journal of Physical Chemistry C 112 (2008) 1552.
- [16] C.B. Almquist, P. Biswas, Applied Catalysis A: General 214 (2001) 259.
- [17] P. Boarini, V. Carassiti, A. Maldotti, R. Amadelli, Langmuir 14 (1998) 2080.
- [18] M.A. Brusa, M.A. Grela, Journal of Physical Chemistry B 109 (2005) 1914.
- [19] A.Y. Nosaka, et al. Journal of Physical Chemistry B 107 (2003) 12042.
- [20] J. Soria, et al. The Journal of Physical Chemistry C 111 (2007) 10590.
- [21] N. Sakai, A. Fujishima, T. Watanabe, K. Hashimoto, Journal of Physical Chemistry B 107 (2003) 1028.
- [22] R. Wang, et al. The Journal of Physical Chemistry B 103 (1999) 2188.
- [23] T.A. Nijhuis, B.M. Weckhuysen, Catalysis Today 117 (2006) 84.
- [24] D. Panayotov, J.T. Yates, Journal of Physical Chemistry B 107 (2003) 10560.
- [25] I. Langmuir, Journal of the American Chemical Society 38 (1916) 2221.
- [26] C.B. Mendive, T. Bredow, M.A. Blesa, D.W. Bahnemann, Physical Chemistry Chemical Physics 8 (2006) 3232.